Effect of the nonlinearity of the CCD in Fourier transform profilometry on spectrum overlapping and measurement accuracy*

Qiao Nao-Sheng(乔闹生)[a)b)] and Zou Bei-Ji(邹北骥)[a)†]

[a)] School of Information Science and Engineering, Central South University, Changsha 410083, China
[b)] School of Physics and Electronics, Hunan University of Arts and Science, Changde 415000, China

(Received 30 May 2012; revised manuscript received 15 June 2012)

In Fourier transform profilometry (FTP), we must restrain spectrum overlapping caused by the nonlinearity of the charge coupled device (CCD) and increase the measurement accuracy of the object shape. Firstly, the causes of producing higher-order spectrum components and inducing spectrum overlapping are analysed theoretically, and a simple physical explanation and analytical deduction are given. Secondly, aiming to suppress spectrum overlapping and improve measurement accuracy, the influence of spatial carrier frequency of projection grating on them is analysed. A method of increasing the spatial carrier frequency of projection grating to restrain or reduce the spectrum overlapping significantly is proposed. We then analyze the mechanism of how the spectrum overlapping is reduced. Finally, the simulation results and experimental measurements verify the correction of the proposed theory and method.

Keywords: spectra overlapping, measurement accuracy, nonlinearity of CCD, Fourier transform profilometry

PACS: 42.30.–d, 42.30.Kq, 42.30.Wb **DOI:** 10.1088/1674-1056/22/1/014203

1. Introduction

Fourier transform profilometry (FTP) based on fringe projection of grating has been widely used in machine vision, solid modeling, industrial auto-measuring, etc.[1–4] When it is used to measure object height, under ideal conditions, there may exist a direct proportional relationship between the light intensity output and that of the input in dynamic scope of the charge coupled device (CCD).[5–7] However, under the actual conditions, because of the nonlinearity of CCD, when we use a CCD camera to acquire the deformed fringe of the object surface and then to carry, the Fourier transformation,[8–10] may include not only the first-order spectra but also the second-order and third-order spectra and so on among spectrum distribution, leading to the spectrum overlapping phenomenon. Therefore, not only the application scope of the method is restricted, but also the measurement accuracy of the object shape is reduced.

Aiming at the importance of extracting useful height information and increasing the measurement accuracy of object shape by using the FTP method, we must try our best to restrain or reduce spectrum overlapping. In this paper, the theory concerning spectrum overlapping caused by the nonlinearity of the CCD is analysed in detail. The influence of spatial carrier frequency of projection grating on spectrum overlapping and measurement accuracy are discussed. A method is proposed which increases the spatial carrier frequency of projection grating, and can restrain or reduce the spectra overlapping as much as possible, and it can increase the measurement accuracy using this method. Computer simulations and practical measurements verify the correction of the theory and method proposed above.

2. Theoretical analysis

2.1. Spectrum overlapping caused by the nonlinearity of the CCD

The CCD is a semiconductor photoelectric device that can convert light energy into electric energy. Under ideal conditions, there may exist a linear relationship between output light intensity and input light intensity of the CCD. Supposing that the y axis is fixed, we can obtain the deformed fringe light intensity from the CCD camera system as follows:

$$g(x,y) = a(x,y) + b(x,y)\cos[2\pi f_0 x + \phi(x,y)], \qquad (1)$$

where $a(x,y)$ is the background light intensity, $b(x,y)$ is the fringe contrast, f_0 is the spatial carrier frequency of projection grating along the x axis, and $\phi(x,y)$ is the phase modulation caused by height distribution $h(x,y)$. According to Ref. [11], the relationship between $\phi(x,y)$ and $h(x,y)$ is $\phi(x,y) = -2\pi f_0 d L_0^{-1} h(x,y)$, where d is the distance between P_2 and I_2, and L_0 is the distance between I_2 and O.

When a one-dimensional (1D) fast Fourier transform algorithm is applied to the deformed fringe light intensity as mentioned above along the x axis, the spectrum distribution can be obtained as follows:

$$G(f,y) = A(f,y) + C(f - f_0, y) + C^*(f + f_0, y), \qquad (2)$$

*Project supported by the National Natural Science Foundation of China (Grant Nos. 61173122, 60970098, 60803024, 90715043, and 61144006) and the Postdoctoral Startup Foundation of Central South University, China (Grant No. 1332/74341016030).

†Corresponding author. E-mail: bjzou@vip.163.com

© 2013 Chinese Physical Society and IOP Publishing Ltd

where $A(f,y)$ is the zero-order spectrum component which can be eliminated by π phase shifting technology,[12–14] $C(f-f_0,y)$ and $C^*(f+f_0,y)$ are first-order spectrum components which contain object height information.

Under the actual conditions, a nonlinear relationship may exist between output light intensity and input light intensity of the CCD, and it usually has second-order and third-order nonlinearity, which may lead to a "double frequency phenomenon" among spectrum distribution, so the deformed fringe light intensity observed through a CCD camera can usually be expressed as follows:

$$g'(x,y)=\sum_{n=0}^{3}e_n g^n(x,y), \tag{3}$$

where e_0, e_1, e_2, and e_3 are constant, first-order, second-order, and third-order response coefficients, respectively.

From Eqs. (1) and (3), we can obtain

$$\begin{aligned} g'(x,y) &= k_0+k_1\exp(\mathrm{i}2\pi f_0 x)+k_2\exp(\mathrm{i}4\pi f_0 x)\\ &\quad +k_3\exp(\mathrm{i}6\pi f_0 x)+k_1^*\exp(-\mathrm{i}2\pi f_0 x)\\ &\quad +k_2^*\exp(-i4\pi f_0 x)+k_3^*\exp(-i6\pi f_0 x), \end{aligned} \tag{4}$$

where k_0, k_1, k_2, k_3, k_1^*, k_2^*, and k_3^* are relational coefficients.

Equation (4) can be converted into the frequency domain by the Fourier transform as follows:

$$\begin{aligned} G'(f,y) &= k_0'(f,y)+k_1'(f-f_0,y)+(k_1^*)'(f+f_0,y)\\ &\quad +k_2'(f-2f_0,y)+(k_2^*)'(f+2f_0,y)\\ &\quad +k_3'(f-3f_0,y)+(k_3^*)'(f+3f_0,y). \end{aligned} \tag{5}$$

It can be seen that Eq. (5) has increased some higher-order spectra such as the second-order spectrum component $k_2'(f-2f_0,y)+(k_2^*)'(f+2f_0,y)$ and the third-order spectrum component $k_2'(f-3f_0,y)+(k_2^*)'(f+3f_0,y)$. These higher-order spectrum components may overlap with the first-order spectrum component of the adjacent frequency island, and this may lead to the spectrum overlapping phenomenon.

2.2. Influence of spatial carrier frequency of projection grating

There are two kinds of spectrum overlap, one is produced by each order of spectrum situated in the same period, the other is produced by a "frequency island" caused by a lacking sample.[15,16] However, the latter can satisfy the conditions of the sample by using a CCD with higher resolving power to acquire a deformed fringe, namely, the number of samples in one period must exceed 4.[15,16] Because the object height information is contained in the first-order spectra, we may only discuss the spectrum overlapping between the first-order spectrum component f_1 and other components under the first condition.

In general, the instantaneous frequency in the nth-order spectrum component along the x axis can be calculated as follows:[11]

$$\begin{aligned} f_n &= \frac{1}{2\pi}\frac{\partial[2\pi n f_0 x+n\phi(x,y)]}{\partial x}\\ &= nf_0+\frac{n}{2\pi}\frac{\partial\phi(x,y)}{\partial x}. \end{aligned} \tag{6}$$

The overlapping between the first-order spectrum component f_1 and other components must be avoided, namely, the first-order spectrum component must be separated from other higher-order spectrum components, so the following expressions must be satisfied:

$$\begin{cases} (f_1)_{\max}<(f_n)_{\min}, \\ (f_{\mathrm{L}})_{\max}<(f_1)_{\min}, \end{cases} \quad (n=2,3,\ldots), \tag{7}$$

where f_{L} is zero-order spectrum.

According to Eqs. (6) and (7), and considering the practical condition of the nonlinearity of the CCD, we can obtain

$$\begin{aligned} &\left|\frac{\partial\phi(x,y)}{\partial x}\right|_{\max}<\frac{n-1}{n+1}2\pi f_0, \quad (n=2,3,\ldots),\\ &\left|\frac{\partial\phi(x,y)}{\partial x}\right|_{\max}<2\pi(f_0-f_{\mathrm{L}}). \end{aligned} \tag{8}$$

In most cases, f_{L} is much lower than $f_0/2$, supposing that the nonlinearity of the CCD is considered, the limit is set by $n>1$ in Eq. (8). Because $(n-1)(n+1)^{-1}$ increases monotonically with increasing n, the phase variation caused by the height modulation must be limited as follows:

$$\left|\frac{\partial\phi(x,y)}{\partial x}\right|_{\max}<\frac{2\pi f_0}{3}. \tag{9}$$

It can be seen from Eq. (9) that we can increase the variation scope of the phase modulation $\phi(x,y)$ when we increase the value of f_0, and we can restrain the spectrum overlapping between the first-order spectrum component and high-order spectrum components from the nonlinearity of the CCD, then the height distribution $h(x,y)$ can be resumed as much as possible so that the measurement accuracy can be increased correspondingly.

The measurement accuracy depends on the equivalent wavelength, while the latter depends on L_0/d and f_0,[11] and their relationship can be expressed as follows:

$$\left|\frac{\partial h(x,y)}{\partial\phi(x,y)}\right|=\frac{L_0}{2\pi f_0 d}. \tag{10}$$

The smaller the value of expression (10) is, the higher the measurement accuracy is. However, the measurement scope can be affected when the value of L_0/d is reduced. Therefore, under the usual conditions, we can keep the resolving power of the CCD unchanged to increase f_0 so as to reduce $|\partial h(x,y)/\partial\phi(x,y)|$, and then the measurement accuracy of the object shape can be increased.

3. Results of spectrum overlapping caused by the nonlinearity of the CCD

3.1. Computer simulation

Supposing that geometry parameter of the measurement system is $L_0/d = 3$, the spatial carrier frequency of the projection grating is $f_0 = 0.1$ mm^{-1}, the simulation object is $h(x,y) = 8\sin(x/100)$, and the deformed fringe light intensity from the ideal CCD camera system is $g(x,y) = 0.5 + 0.5\cos(2\pi f_0 x + \phi(x,y))$.

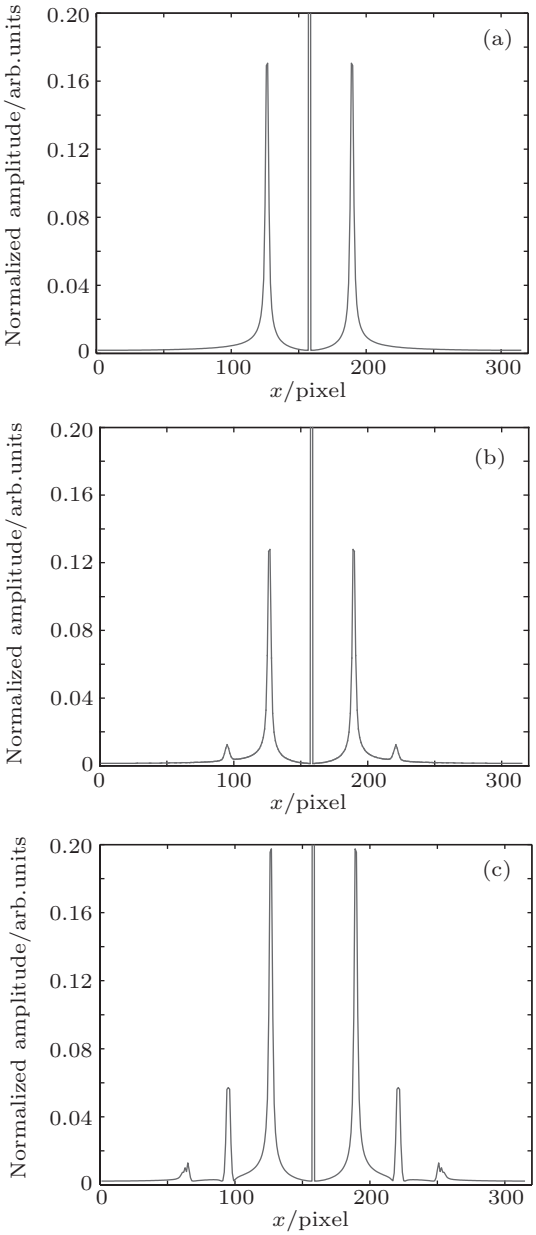


Fig. 1. Simulation results for spectrum distributions of the deformed fringe along the x axis in the presence of (a) linearity, (b) second-order nonlinearity, and (c) third-order nonlinearity.

When a Fourier transform is applied to the linearity light intensity output $g_1(x,y) = 0.12 + 1.23g(x,y)$, we can obtain the spectrum distribution of the deformed fringe along the x axis as shown in Fig. 1(a), and it can be seen that there are only relatively separate zero-order spectrum and first-order spectrum components.

Supposing that there exists second-order and third-order nonlinearity in the CCD, the light intensity output is

$$g_2(x,y) = 0.13 + 1.23g(x,y) - 0.41g^2(x,y),$$
$$g_3(x,y) = 0.12 + 0.61g(x,y) - 1.16g^2(x,y) + 1.23g^3(x,y),$$

respectively. When the Fourier transform is applied to them, we can obtain the spectrum distribution of the deformed fringe along the x axis is shown in Figs. 1(b) and 1(c), respectively. It can be seen clearly from the two figures that they include not only the first-order spectrum component but also the second-order and third-order spectrum components, and they may lead to the overlapping phenomenon among spectrum components.

3.2. Experiment

Experimental measurement is carried out using a mask of a man face. A schematic diagram of the simple experimental equipment is shown in Fig. 2, and the geometry parameters of measurement system are $L_0 = 900$ mm and $d = 400$ mm, the experimental results are 26 deformed fringes and 512×512 pixels.

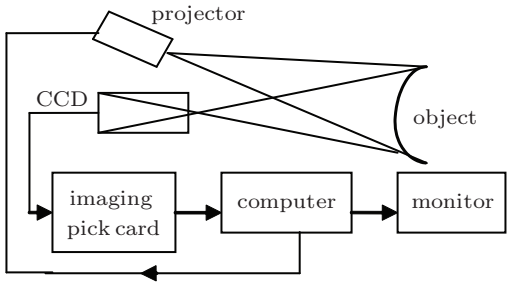


Fig. 2. Schematic diagram of experimental equipment.

When these fringes are sampled, we can obtain the deformed fringe pattern with 256×256 pixels, as shown in Fig. 3(a), so it contains 9.8462 pixels in each period, and it can satisfy the conditions of sampling.[15,16] When the Fourier transform is applied to these deformed fringes, we can obtain the spectrum distribution of fringes along the x axis as shown in Fig. 3(b), and it can be seen clearly that there are overlapping phenomena between the first-order spectrum component and the adjacent periodic higher-order spectrum components due to the nonlinearity of the CCD under the actual conditions.

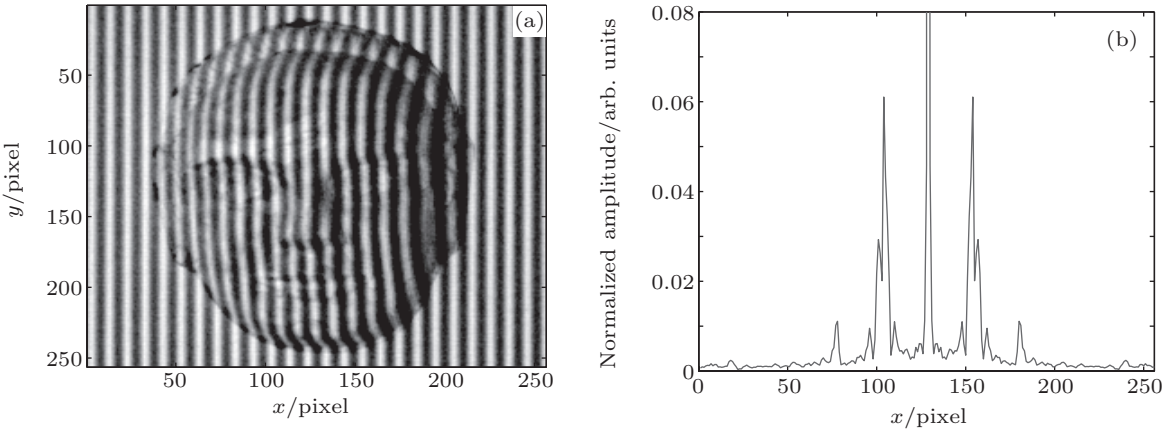


Fig. 3. Experimental results of (a) deformed fringe pattern of the object surface, and (b) spectrum distribution of the deformed fringe of the object surface along the x axis.

4. Results of the influence of spatial carrier frequency of projection grating

4.1. Computer simulation

Supposing that the geometry parameter of a measurement system is $L_0/d = 9/4$ and the spatial carrier frequency of projection grating is $f_0 = 1/12$ mm^{-1}, then the deformed fringe light intensity from the ideal CCD camera system is

$$g(x,y) = 0.5 + 0.5\cos(2\pi f_0 x + \phi(x,y)),$$

while that from the CCD camera system is

$$g_1(x,y) = 0.17 - 0.33g(x,y) + 3.03g^2(x,y) - 1.21g^3(x,y).$$

The simulation object is located in the centre of the projection field, and the maximum value and mean value of the object height are 3.8313 and 0.3606 mm, respectively.

We can obtain the deformed fringe pattern of the object surface through projection grating as shown in Fig. 4(a) ($n = 256$). When we apply the Fourier transform, rectangle filter and reverse Fourier transform to $g_1(x,y)$, we can obtain the spectra distribution along the x axis as shown in Fig. 4(b), and the absolute height error of the object surface as shown in Fig. 4(c). Calculations indicate that the maximum absolute height error and mean absolute height error between the measured value and the actual value are 0.0558 and 0.0157 mm, respectively.

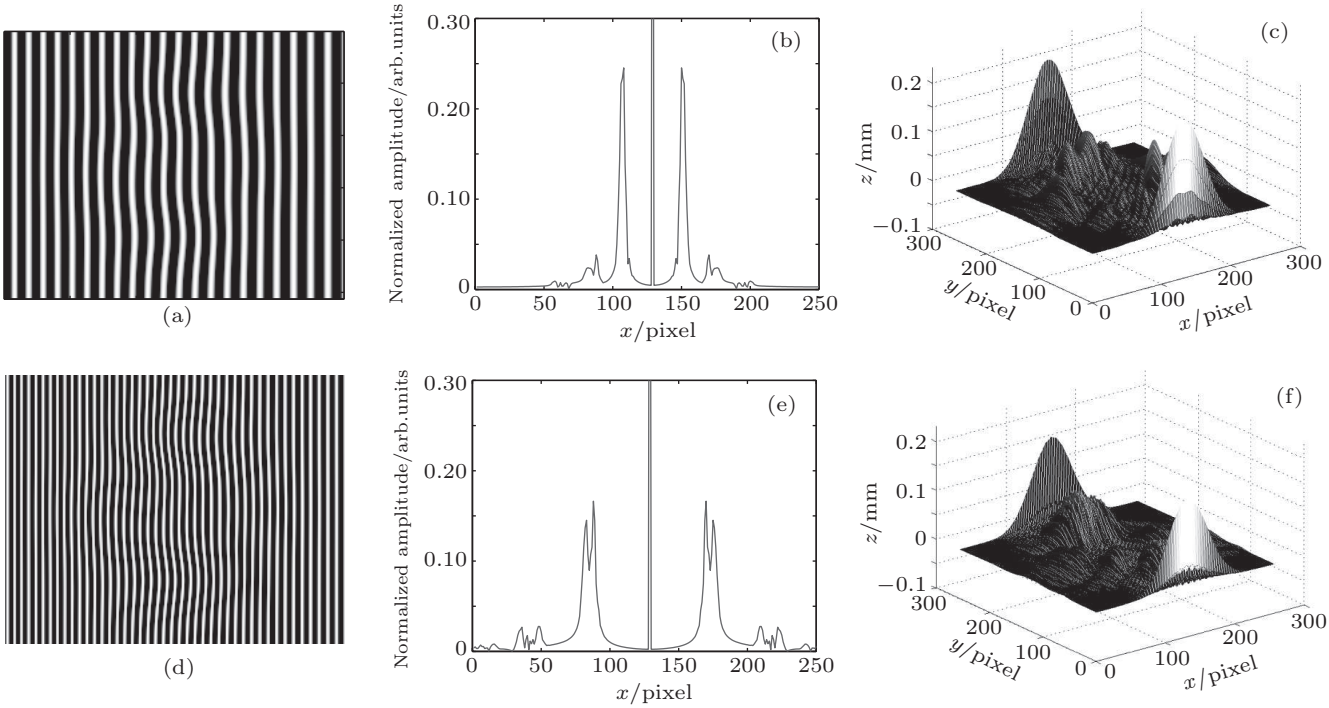


Fig. 4. Simulation results of (a) the deformed fringe pattern based on $f_0 = 1/12$, (b) the spectrum distribution of deformed fringes along the x axis based on $f_0 = 1/12$, (c) the absolute height error between the measured value and the actual value based on $f_0 = 1/12$, (d) the deformed fringe pattern based on $f_0 = 1/6$, (e) the spectrum distribution of the deformed fringe along the x axis based on $f_0 = 1/6$, and (f) the absolute height error between the measured value and the actual value based on $f_0 = 1/6$.

Now we keep the geometry parameter of the measurement system unchanged, the spatial carrier frequency of projection grating is increased to $f_0' = 1/6$ mm^{-1}, and the resolving power of the CCD is increased at the same time. When we use the same object located in the centre of the projection field, we can obtain a corresponding deformed fringe pattern, the spectrum distribution along the x axis, and absolute height errors of the object as shown in Figs. 4(d)–4(f), respectively.

When the geometry parameters of the measurement system are kept unchanged while the spatial carrier frequency of the projection grating is increased, we can see from Fig. 4 that the spectrum overlapping between the first-order spectrum component and the higher-order spectrum components caused by the nonlinearity of the CCD is obviously reduced or restrained, and then it can create good conditions for the improvement on measurement accuracy. By calculation, the maximum absolute height error and mean absolute height error between the measured value and the actual value are 0.0367 and 0.0100 mm, respectively.

4.2. Experiment

In order to further verify the validity of the theory and method, we design a practical experiment. By using the simple experimental equipment as shown in Fig. 2, we can obtain the deformed fringe patterns of the lower and the higher spatial carrier frequency of the projection grating as shown in Figs. 5(a) and 5(d), respectively. The spectrum distributions obtained after Fourier transform in the deformed fringes of the lower and the higher spatial carrier frequency are shown in Figs. 5(b) and 5(e), respectively. It can be seen that the separation result between the first-order spectrum component and the higher-order spectrum components as shown in Fig. 5(e) is better than that in Fig. 5(b), namely, the spectrum overlapping by adopting a higher spatial carrier frequency is restrained better than that that which adopts the lower spatial carrier frequency. The object heights resumed by using the lower and the higher spatial carrier frequency of the projection grating are shown in Figs. 5(c) and 5(f), respectively. It can be seen that the resumption result as shown in Fig. 5(f) is better than that in Fig. 5(c).

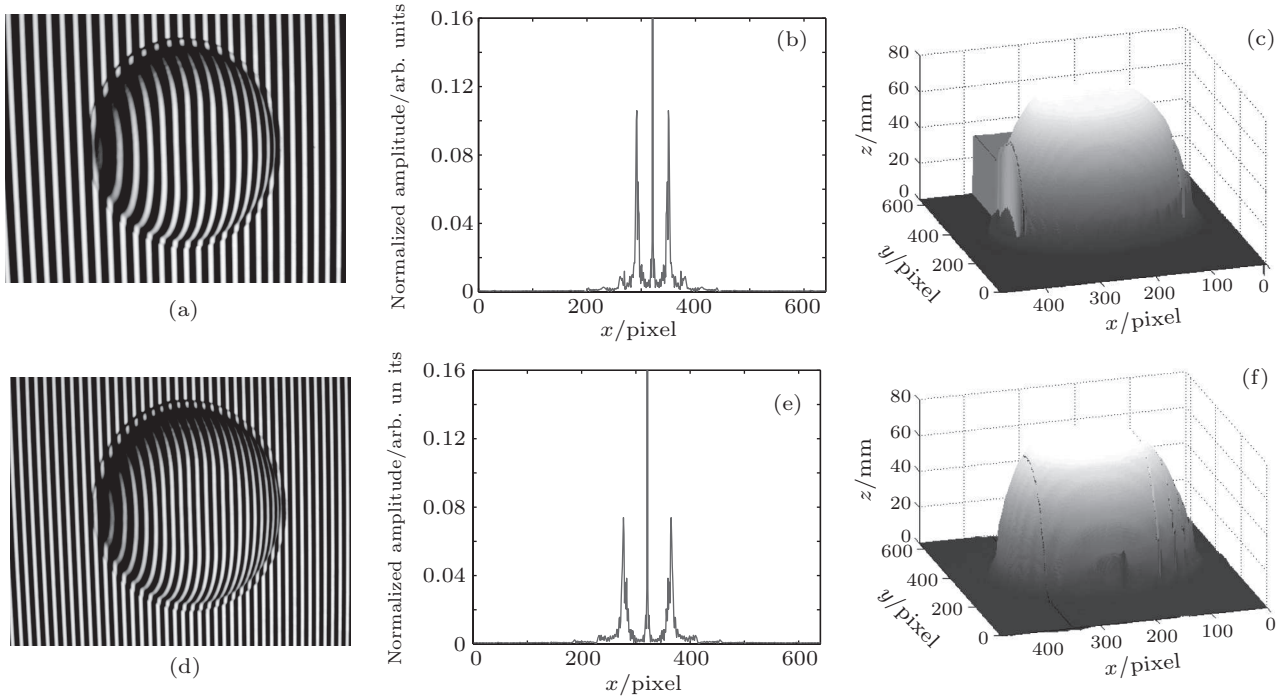


Fig. 5. Experimental results showing (a) the deformed fringe pattern of the lower spatial carrier frequency, (b) the spectrum distribution of the deformed fringe of the object surface by using the lower spatial carrier frequency along the x axis, (c) the object height resumed by using the lower spatial carrier frequency, (d) the deformed fringe pattern of the higher spatial carrier frequency, (e) spectra distribution of the deformed fringe of the object surface by using the higher spatial carrier frequency along the x axis, and (f) object height resumed by using the higher spatial carrier frequency.

5. Conclusions

Owing to the nonlinearity of the CCD, the causes of producing higher-order spectrum components and leading to spectrum overlapping with the first-order spectrum component are analysed theoretically, and a simple physical explanation and analytical deduction are given. The influences of spatial carrier frequency of projection grating on spectrum overlapping and measurement accuracy are analysed. A method of restraining or reducing the spectrum overlapping by increasing

the spatial carrier frequency of projection grating is proposed. Moreover, we point out that one can increase the measurement accuracy of the object shape by using the method.

We use computer simulations and practical experiments to prove the theory and method proposed in this paper. The results verify the correctness of the analysis and deduction.

References

[1] Xu J L, Wang M, Pan H, Liu X H, Qi X L and Xu S X 2011 *Acta Phys. Sin.* **60** 074210 (in Chinese)
[2] Qiao N S, Cai X H and Yao C M 2009 *Chin. Phys.* B **18** 4881
[3] Cui S L, Tian F and Li D H 2012 *Appl. Opt.* **51** 3194
[4] Wen Y F, Li S K, Cheng H B, Su X Y and Zhang Q C 2010 *Appl. Opt.* **49** 6563
[5] Wang D J and Zhang T 2011 *Chin. Phys.* B **20** 087202
[6] Pei L, Liu G H, Ning T G, Gao S, Li J and Zhang Y J 2012 *Acta Phys. Sin.* **61** 064203 (in Chinese)
[7] Liu G H, Pei L, Ning T G, Gao S, Li J and Zhang Y J 2012 *Acta Phys. Sin.* **61** 094205 (in Chinese)
[8] Fan T Y, Xie L Y, Fan L and Wang Q Z 2011 *Chin. Phys.* B **20** 076102
[9] Lü C H, Fan H Y and Jiang N Q 2010 *Chin. Phys.* B **19** 120303
[10] Shi P, Cao G W and Li Y P 2010 *Chin. Phys.* B **19** 074201
[11] Takeda M and Mutoh K 1983 *Appl. Opt.* **22** 3977
[12] Chatterjee S and Kumar Y P 2011 *Opt. Commun.* **284** 57
[13] Stoykova E, Gotchev A and Sainov V 2011 *Opt. Commun.* **284** 88
[14] Yookas T and Lwaasa Y 1986 *Appl. Opt.* **25** 1630
[15] Qiao N S, Cai X H, Peng G H and Liu H Q 2006 *J. Opt. Laser* **17** 1339 (in Chinese)
[16] Chen W J, Li M H and Su X Y 2009 *Optik.* **120** 652